

Accepted Manuscript

Design, Synthesis and Antitumor Activity of Novel Sorafenib Derivatives Bearing Pyrazole Scaffold

Min Wang, Shan Xu, Huajun Lei, Caolin Wang, Zhen Xiao, Shuang Jia, Jia Zhi, Pengwu Zheng, Wufu Zhu

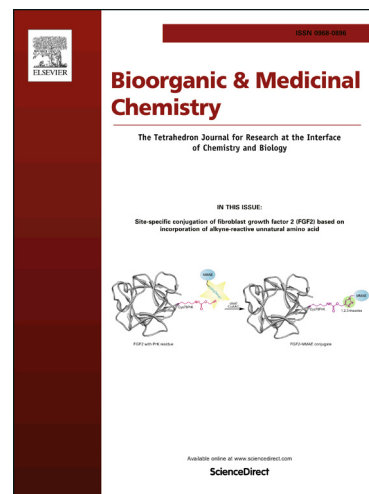
PII: S0968-0896(17)31277-4
DOI: <http://dx.doi.org/10.1016/j.bmc.2017.09.003>
Reference: BMC 13963

To appear in: *Bioorganic & Medicinal Chemistry*

Received Date: 21 June 2017
Revised Date: 29 August 2017
Accepted Date: 4 September 2017

Please cite this article as: Wang, M., Xu, S., Lei, H., Wang, C., Xiao, Z., Jia, S., Zhi, J., Zheng, P., Zhu, W., Design, Synthesis and Antitumor Activity of Novel Sorafenib Derivatives Bearing Pyrazole Scaffold, *Bioorganic & Medicinal Chemistry* (2017), doi: <http://dx.doi.org/10.1016/j.bmc.2017.09.003>

This is a PDF file of an unedited manuscript that has been accepted for publication. As a service to our customers we are providing this early version of the manuscript. The manuscript will undergo copyediting, typesetting, and review of the resulting proof before it is published in its final form. Please note that during the production process errors may be discovered which could affect the content, and all legal disclaimers that apply to the journal pertain.



Design, Synthesis and Antitumor Activity of Novel Sorafenib Derivatives Bearing Pyrazole Scaffold

Min Wang[†], Shan Xu[†], Huajun Lei[†], Caolin Wang, Zhen Xiao, Shuang Jia, Jia Zhi, Pengwu Zheng*, Wufu Zhu*¹

Jiangxi Provincial Key Laboratory of Drug Design and Evaluation, School of Pharmacy, Jiangxi Science & Technology Normal University, Nanchang 330013, P.R. China

Abstract: Four series of Sorafenib derivatives bearing pyrazole scaffold (**8a–m**, **9a–c**, **10a–e** and **11a**) were synthesized and characterized by NMR and MS. All of the target compounds were evaluated for the cytotoxicity against A549, HepG2, MCF-7, and PC-3 cancer cell lines and some selected compounds were further evaluated for the activity against VEGFR-2/KDR, BRAF, CRAF, c-Met, EGFR and Flt-3 kinases. Compounds **8b** and **8i** were more active than that of compounds **8h**, **9a**, especially the IC₅₀ value of compounds **8b** on VEGFR-2 kinase was 0.56 μM. And compound **8b** exhibited moderate to good activity toward c-Met and showed moderate to no activity against CRAF, c-Met, EGFR, Flt-3 kinases. Eleven of the target compounds exhibited moderate to good antitumor activities. The most promising compound **8b** showed strong antitumor activities against A549, HepG2 and MCF-7 cell lines with IC₅₀ values of 2.84±0.78 μM, 1.85±0.03 μM and 1.96±0.28 μM, which were equivalent to sorafenib (2.92±0.68 μM, 3.44±0.50 μM and 3.18±0.18 μM). Structure–activity relationships (SARs) and docking studies indicated that the pyrazole scaffolds exerted key effect on antitumor activities of target compounds. Substitutions of aryl group at C-3 positions had a significant impact on the antitumor activities, and 3-Br substitution produced the best potency.

Key words: Sorafenib derivatives; Pyrazole, VEGFR-2/KDR kinase inhibitors; Anticancer activity

[†] These authors contribute equally to this work

Corresponding author. Tel./fax: +86 791 83802393.

E-mail address: zhengpw@126.com, zhuwuf@jxstnu.edu.cn, zhuwufu-1122@163.com (W. Zhu).

1. Introduction

Cancer is a widespread, complex, and lethal disease. And its burden is increasing across the world dramatically. It is considered as the first leading cause of deaths in economically developed countries and the second leading cause of deaths in developing countries^[1]. Despite the rapid progress in medicine, the commitment to the laborious task of discovering new anticancer agents remains critically important^[2]. Transformed cells secrete a cocktail of pro-angiogenic proteins including vascular endothelial growth factors (VEGFs) and fibroblast growth factors (FGFs) in the process of tumor growth. So in recent years, VEGF has been the key anti-tumor angiogenesis therapy Targets. The family members of VEGFR mainly contain VEGFR-1, VEGFR-2 and VEGFR-3. Among them, VEGFR2 is a key mediator of pro-angiogenic signalling in the endothelium, which can adjust the lymphatic endothelial cells and vascular endothelial cells, and promote the formation of lymphatic and blood vessels, and adjust the migration of lymphocytes, and so on. Small-molecule VEGFR2 inhibitors (ATP analogues) were some of the first treatments to show anti-angiogenic efficacy with clinical benefits for cancer patients. The Ras/RAF/MEK/ERK mitogen-activated protein kinase (MAPK) signaling pathway plays an important role in the transduction of signals from cell surface receptors to the nucleus, like regulating cell growth, survival, differentiation and proliferation in response to external stimuli (growth factors, cytokines or hormones)^[3-4]. Sorafenib (BAY 43-9006; Nexavar)^[3-4] is a bis-aryl urea, which can inhibit the Ras / Raf / MEK signal transduction pathway and also can block the formation of new blood vessels by suppressing the receptor protein of VEGFR and PDGFR. Thus, it inhibits the growth of tumor cells^[5-9].

The preliminary study showed that the urea structure was very important for its biological activity, and NH atoms can play an important role in the formation of hydrogen bonds with amino acid residues. In recent years, compounds containing pyrazole are widely used in biology^[10-12], pharmacology^[13-14], food^[15], agrochemical fields^[16] and so on. And many pyrazole derivatives were reported, such as compound I, II, III, IV and V (The structures were shown in Figure 1)^[17-21] and these compounds elicited strong cytotoxic activity. The results showed that the pyrazole scaffold played a key role to the activity. Encouraged by this, we replaced the urea with pyrazole yielding compounds **8a-m**. In order to investigate the effect of the position of carbon-nitrogen double bond to the activity of the compounds, we designed compounds **9a-c**. It is proposed to introduce thioamide at carbon-nitrogen single bond and got two series compounds (**10a-e**, **11a**) for the purpose of making

the sorafenib derivatives binding with receptor more closely, which was effected by active pharmacophore of urea. Then we disclosed the synthesis and antitumor activity against A549, PC-3, MCF-7, and HepG2 cancer cell lines, and VEGFR-2 kinase of target compounds (see Fig. 1). Moreover, docking studies were presented in this paper as well.

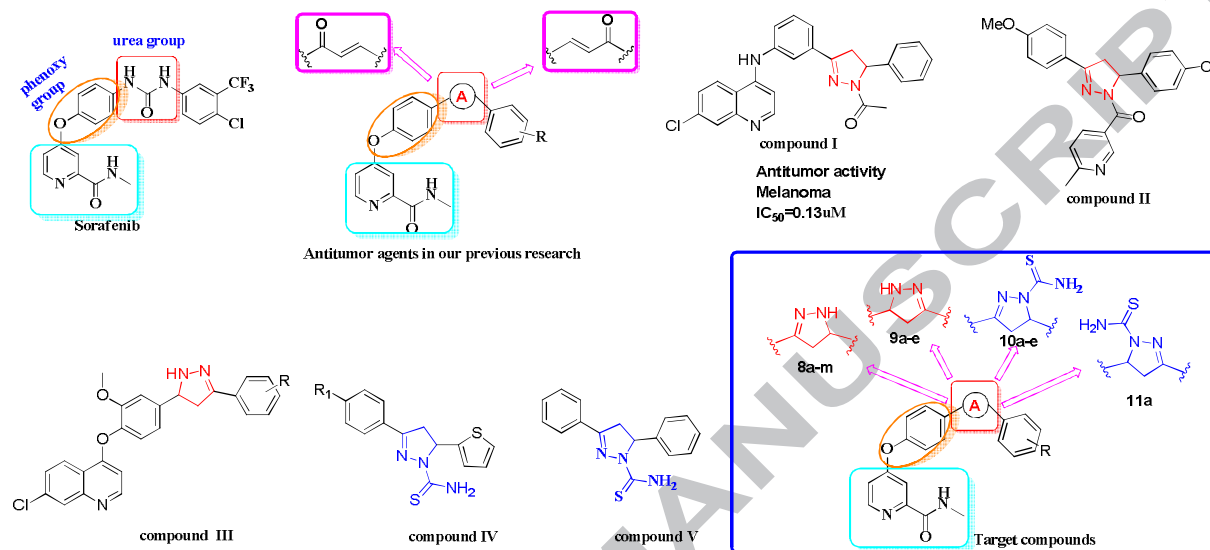
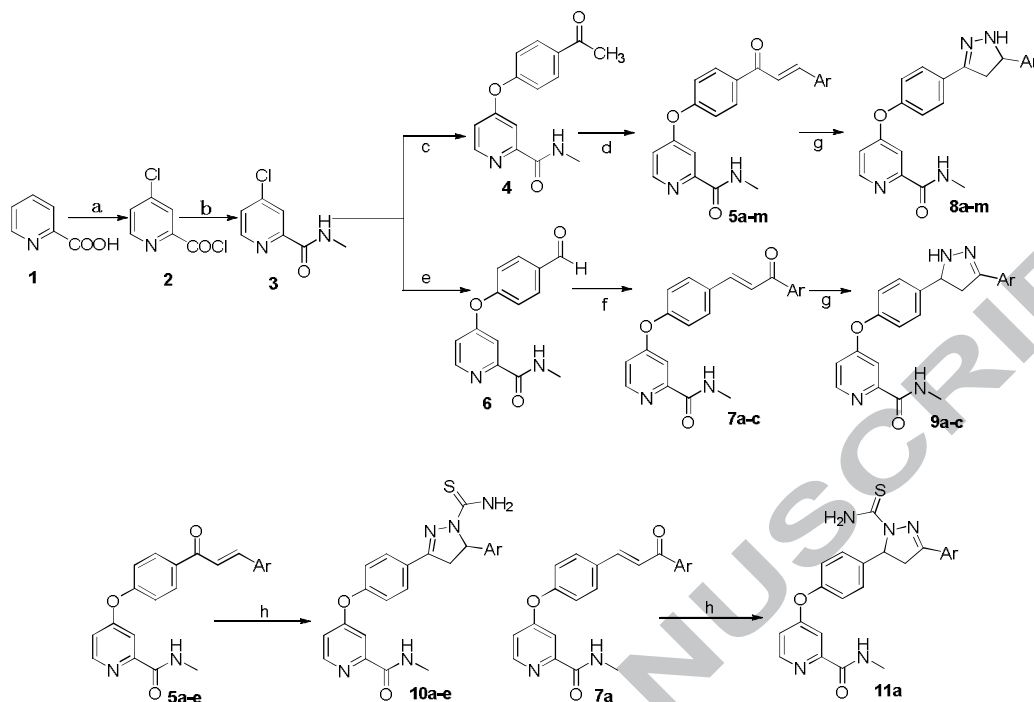


Figure 1. Structures of small-molecule antitumor agents and target compounds (8a–m, 9a–c, 10a–e and 11a).

2. Chemistry

The preparation of target compounds **8a–m**, **9a–c**, **10a–e** and **11a** was described in Scheme 1. Compounds **2** and **3** were synthesized according to the reported procedures [22]. Subsequently, 1-(4-hydroxyphenyl)ethanone, 4-chloro-*N*-methylpicolinamide (**3**) and K_2CO_3 were added in DMSO, which was refluxed for about 5 h in three neck flask and yielded the key compound 4-(4-acetylphenoxy)-*N*-methylpicolinamide(**4**). The other intermediate 4-(4-formylphenoxy)-*N*-methylpicolinamide (**6**) was achieved from 4-chloro-*N*-methylpicolinamide (**3**) via substitution reaction with 4-hydroxybenzaldehyde and potassium tert-butoxide. 4-(4-acetylphenoxy)-*N*-methylpicolinamide(**4**)[intermediate 4-(4-formylphenoxy)-

N-methylpicolinamide (**6**)] was reacted with substituted benzaldehyde (substituted acetophenone) through aldol condensation to get the compound **5a–m** (**7a–c**). Finally, the compound **5a–m** (**7a–c**) with hydrazine hydrate(80%) in acetic acid at 108 °C for 1 h through addition reaction yielded target compounds **8a–m** and **9a–c** respectively. And we were used compound **5a–e** (**7a**) in an addition reaction with thiosemicarbazide to generate target compounds **10a–e** and **11a**.



Reagents and conditions: (a) SOCl_2 , NaBr, chlorobenzene, 85 °C, 20 h; (b) 30% MeNH_2 , toluene, 20 °C, 6 h; (c) K_2CO_3 , DMSO, reflux, 5h; (d) KOH, methanol, r.t 6 h. (e) *tert*-BuOK, DMF, reflux, 15 h; (f) NaH, THF, r.t 8 h; (g) hydrazine hydrate, acetic acid, reflux, 2.5 h; (h) thiosemicarbazide, KOH, ethanol, microwave, 100 W ,60 °C, 15 min.

Scheme 1. Synthetic route of target compounds.

3. Results and discussion

3.1. Biological evaluation

Selecting A549 (human lung cancer), PC-3 (human prostatic cancer), MCF-7 (human breast cancer) and HepG2 (human liver cancer) with high expression of VEGFR-2 kinase as tested cancer lines, the target compounds (**8a–m**, **9a–c**, **10a–e** and **11a**) were evaluated for the cytotoxicity against four cancer cell lines by 3-(4,5-dimethylthiazolyl-2)-2,5-diphenyltetrazolium bromide (MTT) cell proliferation assay, using Sorafenib as lead compound. In addition, some selected compounds were evaluated for the IC_{50} values against VEGFR-2 kinase *in vitro* by the mobility shift assay, together with reference compound Sorafenib. The results expressed as IC_{50} values were summarized in Tables 1–3 and the values are the average of at least two independent experiments.

As shown in Tables 1–2, the activity of the first and the second series (**8a–m**, **9a–c**) is much better than that of the third and fourth series (**10a–e**, **11a**). And twelve of the compounds exhibited

excellent cytotoxicity activity against different cancer cells with potency from the single-digit nanomole to μM range. Among them, compounds **8b**, **8i** and **10d** showed superior activity to positive control Sorafenib against one or more cancer cell lines. The most promising compound **8b** exhibits the best activity against A549, HepG2 and MCF-7 cell lines with IC_{50} values of $2.84\pm 0.78 \mu\text{M}$, $1.85\pm 0.03 \mu\text{M}$ and $1.96\pm 0.28 \mu\text{M}$, which were equivalent to Sorafenib ($2.92\pm 0.68 \mu\text{M}$, $3.44\pm 0.50 \mu\text{M}$, $3.18\pm 0.18 \mu\text{M}$). The results suggested that the replacement of the urea fragment with pyrazole scaffold was benefit for the activity. It also told us that the application of pyrazole scaffold was feasible.

Furthermore, different substitutions of aryl group affected the cytotoxicity of target compounds. The latter two series (**10a–e** and **11a**) of compounds had lower cytotoxicity than the first two series (**8a–m** and **9a–c**) of compounds. It was seem to be that the group Br and Cl at C-3 position or none substituents increased the activity of the target compounds, such as compounds **8b**, **8i** and **10d**. In another way, the strong electron-withdrawing groups such as $-\text{CN}$, NO_2 at C-4 position reduced the activity of the target compounds. This dramatic boost of activity told us that the group Br at C-3 had an obviously impact on the activity.

Activity against VEGFR-2, B-RAF, C-RAF, c-Met, EGFR and Flt-3 kinases of four target compounds were further carried out in this paper to investigate the target of these compounds. In Table 3, obviously, compounds **8b** and **8i** were more active than that of compounds **8h**, **9a**, especially the IC_{50} value of compounds **8b** on VEGFR-2 kinase was $0.56 \mu\text{M}$. And compound **8b** exhibited moderate to good activity toward c-Met and showed moderate to no activity against CRAF, c-Met, EGFR, Flt-3 kinases. The results prompted us that this compound may act through other mechanism.

In order to examine the relationship between the antitumor activity of the compound and the concentrations, we used the method of MTT and selected seven different concentrations. The inhibition rate was measured after 72 h. Though Figure 2, the phenomenon of dose-dependent was observed of representative compound **8b**.

Table 1 Structures and activity of target compounds 8a-m and 9a–c

Compounds No.	Ar	$\text{IC}_{50}(\mu\text{M})^a$			
		A549	HepG2	MCF-7	PC-3
8a		6.93±0.89	ND	ND	7.3±0.26

8b		2.84±0.78	1.85±0.03	1.96±0.28	3.54±0.61
8c		37.14±0.44	24.26±1.32	ND	28.28±1.27
8d		17.36±1.44	14.97±1.33	ND	9.91±1.81
8e		13.69±1.09	11.46±0.2	ND	24.25±2.48
8f		19.53±0.84	NA	ND	NA
8g		ND	26.46±0.91	35.37±1.37	ND
8h		13.14±1.27	9.64±1.01	10.97±1.32	7.74±0.72
8i		8.60±0.09	1.50±0.38	1.24±0.02	4.52±0.34
8j		10.71±1.06	14.43±0.99	ND	36.22±1.44
8k		15.14±0.81	5.28±0.22	9.48±0.23	6.77±0.34
8l		21.04±0.12	57.56±0.99	ND	NA
8m		19.0±1.3	15.65±0.23	9.94±0.17	ND
8n		12.12±0.21	4.99±0.08	ND	ND
9a		ND	28.87±1.75	8.03±0.10	ND
9b		ND	16.89±0.94	15.30±1.10	ND
9c		20.47±0.86	10.88±1.27	15.28±0.66	ND

Sorafenib^b 2.92±0.68 3.44±0.50 3.18±0.18 3.24±0.45

^a The values are an average of two separate determinations;

^b Used as positive controls

^c NA: Not active ($IC_{50} > 50 \mu M$)

^d Not determined.

Table 2 Structures and activity of target compounds 10a-e and 11a

Compounds No.	R	$IC_{50}(\mu M)$ ^a		
		A549	HepG2	PC-3
10a		NA ^c	NA	NA
10b		19.41±0.24	NA	NA
10c		NA	NA	NA
10d		NA	1.89±0.28	15.9±1.33
10e		NA	NA	NA
11a		NA	NA	NA
Sorafenib ^b	-	2.92±0.68	3.44±0.5	3.18±0.18

^a The values are an average of two separate determinations;

^b Used as positive controls

^c NA: Not active ($IC_{50} > 50 \mu M$)

Table 3. Activity against six kinases of four compounds

Comp.No.	$IC_{50}(\mu M)$ ^a					
	VEGFR-2/KDR	BRAF	CRAF	c-Met	EGFR	Flt-3
8b	0.56	3.4	7.9	0.54	>10	5.2
8h	NA ^c	NA	ND	ND	ND	ND
8i	2.3	3.9	ND	ND	ND	ND
9a	NA	NA	ND	ND	ND	ND
Sorafenib b	0.17	0.31	0.12	ND	ND	ND
Staurosporine ^b	0.072	ND ^d	ND	ND	ND	ND

^a The values are an average of two separate determinations;

^b Used as positive controls

^c NA: Not active ($IC_{50} > 50 \mu M$)

^d Not determined.

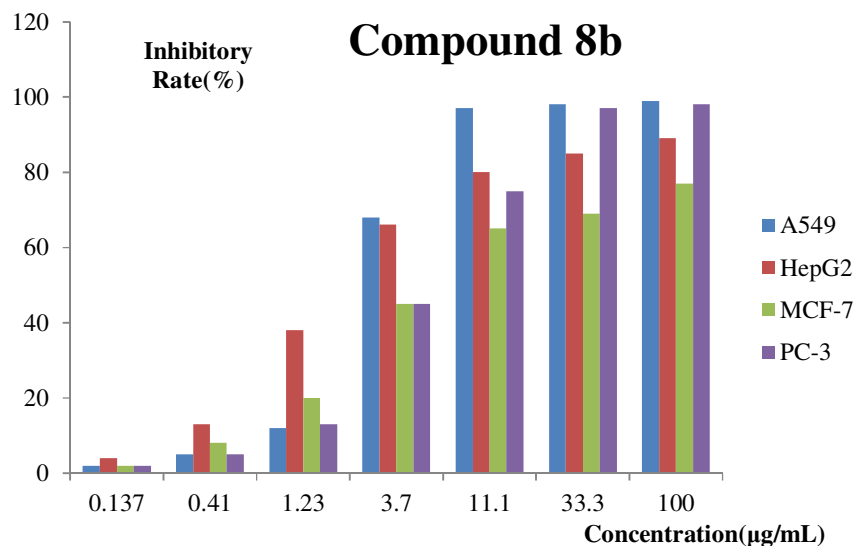


Figure 2 Relationship between activity and concentration of selected compounds 8b against our cancer cell lines

3.2 Compound 8b inhibited the growth of HepG2 cells

As shown in Figure 3, HepG2 cells were treated with compound **8b** (1.04~3.29 $\mu g/mL$) for 24, 48 and 72 h, and cell growth inhibition were determined by MTT assay. Results indicated that compound **8b** inhibited the proliferation of HepG2 cells in a time and concentration-dependent manner in figure 3.

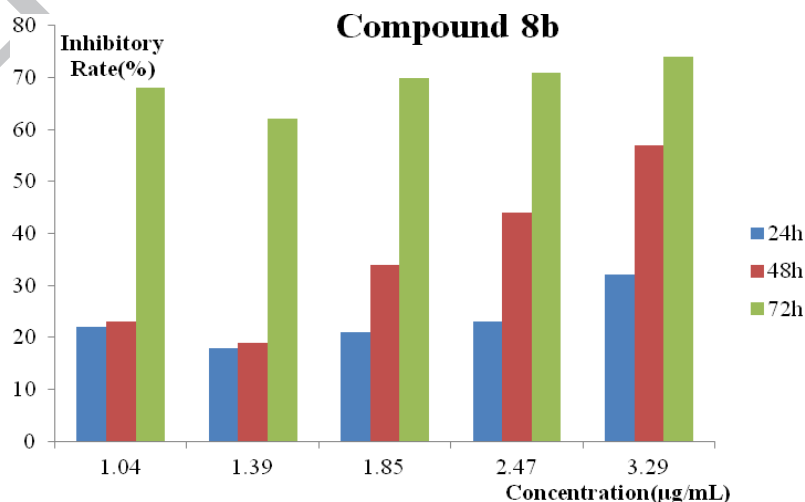


Figure 3 Compound 8b inhibited the growth of HepG2 cells

3.3 Morphologic changes of A549 cells under inverted microscopy and fluorescence Microscopy

We used acridine orange (AO) single staining by MTT method, in the control group [figure 4(a)], we observed the nucleus of A549 cells were stained into green from fluorescence microscopy. And the cells grew well, were full, the edge were clear and the refraction was good. While 1.85 μM concentration of compound **8b** acted on the A549 cell lines after 12 h, the cells shrink, chromatin condensation, the nucleus was dyed bright green, some cells apoptotic bodies and DNA fragments in figure 4(b).

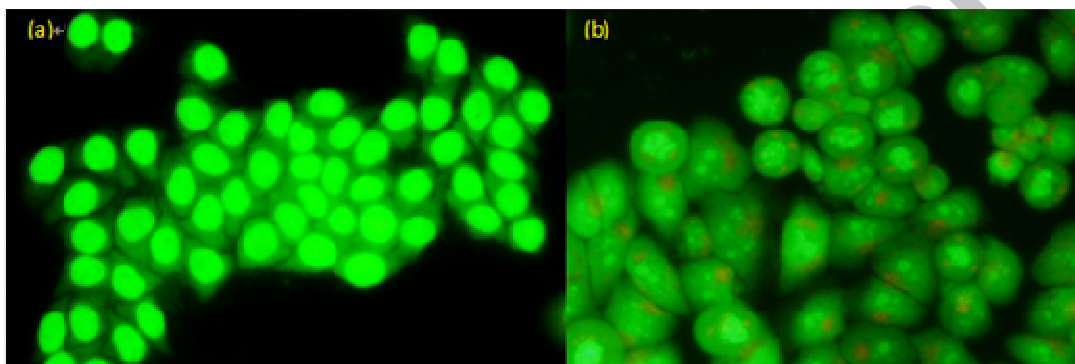


Figure 4 Morphologic changes of A549 cells under inverted microscopy and fluorescence Microscopy

3.4 Apoptosis result by flow cytometry method of operation

According to the apoptosis expression by flow cytometry, the target compounds show cell proliferation activity in another way. To examine whether compound **8b** can induce apoptosis of A549, we adopted flow cytometry method of operation. An obvious reduction in 3 μM , 6 μM and 12 μM concentration was observed respectively. In contrast, no significant change was seen in control group. When the concentration increased to 12 μM , apoptosis emerges more evidently in Figure 5.

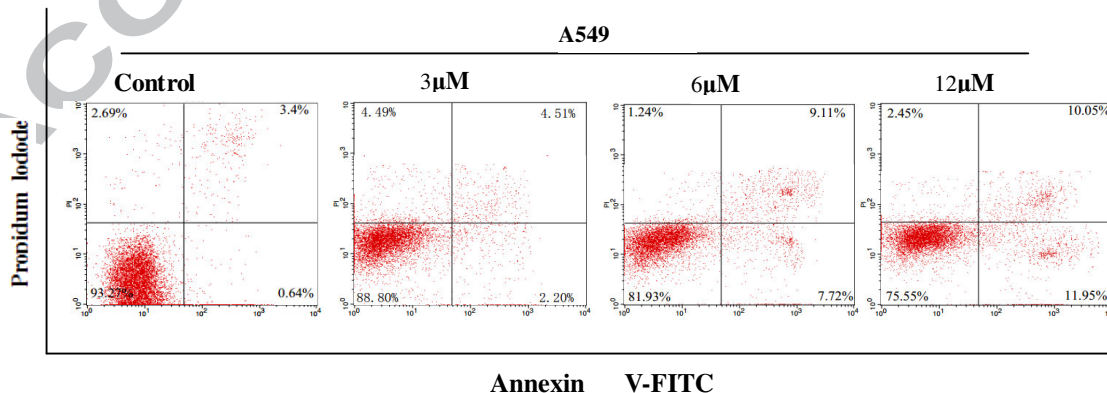


Figure 5 Apoptotic cell death analysis in A549 cells treated with compound **8b**

3.5 Molecular docking study

To explore the binding modes of target compounds with the active site of VEGFR-2 and c-Met, molecular docking simulation studies were carried out by using SURFLEX-DOCK module of SYBYL package version. Based on the *in vitro* inhibition results, we selected compound **8b**, as the ligand example, and the structures of VEGFR-2(PDB ID code: 4ASD) and c-Met (PDB ID code: 3LQ8) were selected as the docking model. The binding modes of compound **8b** and lead compounds were shown in Figure. 6a-d. Analysis of compound **8b** and Sorafenib's binding mode in the active binding site demonstrated that the docking mode of **8b** produced a new H-bond with residues ASN923 of *N*-methylpicolinamide's carbonyl in Figure. 6a, b. The new hydrogen bond really play an important role in increasing the inhibitory potency of pyrazole derivatives against VEGFR-2 kinase according to the docking results. As depicted in Figure. 6c, d, we can see compound **8b** formed three hydrogen bonds with residue MET1160 and LYS1110. Compared with the lead compound, it also produced a new H-bond with residues LYS1110 of Pyrazole. Similarly, The new hydrogen bond really play an important role in increasing the inhibitory potency of pyrazole derivatives against c-Met kinase according to the docking results. Furthermore, the docking results also give us a new direction to design new inhibitors. The above-mentioned results of SARs analysis and molecular docking study may allow the rational design of more potent VEGFR-2 or c-Met inhibitors.

apoptosis or died with the dose of compound **8b** increasing, which indicated the compound **8b** could induce remarkable apoptosis of A549 cells. Further study will be carried out to identify the exact action mechanism in near future.

5. Experimental

5.1. Chemistry

All melting points are obtained on a Büchi Melting Point B-540 apparatus (Büchi Labortechnik, Flawil, Switzerland) and are unchanged. NMR spectra are performed by using Bruker 400 MHz spectrometers (Bruker Bioscience, Billerica, MA, USA) with TMS as an internal standard. Mass spectra (MS) are taken into ESI mode on Agilent 1100 LCMS (Agilent, Palo Alto, CA, USA). All the materials are obtained from commercial suppliers and used without purification, unless otherwise specification. Yields are not optimized. TLC analysis is carried out on silica gel plates GF254 (Qindao Haiyang Chemical, China). All the materials are obtained from commercial suppliers and used without purification, unless otherwise specification. Yields are not optimized.

5.2 General procedure for preparation of compounds **2** and **3**

Compounds **2** and **3** were synthesized according to the reported procedures^[22].

5.3 4-(4-acetylphenoxy)-*N*-methylpicolinamide **4**

A stirring mixture of 1-(4-hydroxyphenyl)ethanone (22 mmol), 4-chloro-*N*-methylpicolinamide (14 mmol) and K₂CO₃ (35 mmol) in DMSO (100 mL) was refluxed for about 5 h in three neck flask. Then the reaction mixture was cooled and cold water was added. The precipitate of 4-(4-acetylphenoxy)-*N*-methylpicolinamide (**4**) formed was filtered. Yield: 32%.

5.4 General procedure for the preparation of compounds **5a–m**

A mixture of 4-(4-acetylphenoxy)-*N*-methylpicolinamide (0.67 mmol) and substituted benzaldehyde (0.67 mmol) were dissolved in methanol (10 mL) and to it 3 mmol of 20% KOH was added. The mixture was kept at room temperature for 6 hours. The solid formed was filtered and washed with isopropanol. No further purification was needed and products were used such as were obtained.

5.5 General procedure for the preparation of compounds **8a–m**

Compounds **5a–m** (0.26 mmol) and hydrazine hydrate (2.4 mmol) were dissolved in acetic acid (10 mL). The mixture was refluxed for 2.5 h with constant stirring. The progress of the reaction

was monitored through TLC. After completion of reaction, mixture was cooled and poured into water, and it was neutralized with potassium carbonate, then it was filtered through vacuum by washing with water.

4-(4-(5-(2,4-dichlorophenyl)-4,5-dihydro-1*H*-pyrazol-3-yl)phenoxy)-*N*-methylpicolinamide(**8a**)

Yield: 75.3%; ESI-MS[M+H]⁺m/z:442.3; m.p.: 129.1-131.0 °C; ¹H NMR (400 MHz, DMSO-*d*₆) δ 8.80 (d, *J* = 4.9 Hz, 1H), 8.54 (d, *J* = 5.6 Hz, 1H), 7.92 (s, 1H), 7.90 (s, 1H), 7.58 (d, *J* = 6.8 Hz, 1H), 7.42 (d, *J* = 2.5 Hz, 1H), 7.33 (dd, *J* = 10.0, 5.8 Hz, 2H), 7.30 (s, 1H), 7.22 (dd, *J* = 5.6, 2.6 Hz, 1H), 7.07 (d, *J* = 7.5 Hz, 1H), 5.80 (dd, *J* = 12.1, 5.0 Hz, 1H), 4.02 (d, *J* = 12.0 Hz, 1H), 3.97 (d, *J* = 11.9 Hz, 1H), 2.78 (d, *J* = 4.8 Hz, 3H).

4-(4-(5-(3-bromophenyl)-4,5-dihydro-1*H*-pyrazol-3-yl)phenoxy)-*N*-methylpicolinamide(**8b**)

Yield: 78.5%; ESI-MS[M+H]⁺m/z:452.3; m.p.: 116.3-117.8 °C; m.p.: 123.3-124.5; ¹H NMR (400 MHz, DMSO-*d*₆) δ 8.80 (d, *J* = 4.7 Hz, 1H), 8.55 (d, *J* = 5.6 Hz, 1H), 7.92 (d, *J* = 8.6 Hz, 1H), 7.45 (dd, *J* = 12.6, 5.3 Hz, 1H), 7.31 (dd, *J* = 12.3, 8.3 Hz, 1H), 7.22 (dd, *J* = 8.8, 5.6 Hz, 1H), 5.56 (dd, *J* = 11.8, 5.0 Hz, 1H), 3.89 (dd, *J* = 15.2, 12.3 Hz, 1H), 3.24 (dd, *J* = 15.3, 5.0 Hz, 1H), 2.78 (d, *J* = 4.8 Hz, 1H).

N-methyl-4-(4-(5-(3,4,5-trimethoxyphenyl)-4,5-dihydro-1*H*-pyrazol-3-yl)phenoxy)picolinamide(**8c**)

Yield: 74.1%; ESI-MS[M+H]⁺m/z:464.2; m.p.: 123.3-124.5 °C; ¹H NMR (400 MHz, DMSO-*d*₆) δ 8.80 (d, *J* = 4.4 Hz, 1H), 8.55 (d, *J* = 5.5 Hz, 1H), 7.91 (d, *J* = 8.7 Hz, 2H), 7.43 (d, *J* = 2.5 Hz, 1H), 7.33 (s, 1H), 7.31 (s, 1H), 7.23 (dd, *J* = 5.6, 2.5 Hz, 1H), 6.48 (s, 2H), 5.49 (dd, *J* = 12.2, 5.1 Hz, 1H), 3.86 (q, *J* = 12.0 Hz, 2H), 3.66 (dd, *J* = 15.5, 15.3 Hz, 9H), 2.78 (d, *J* = 4.8 Hz, 3H).

4-(4-(5-(4-cyanophenyl)-4,5-dihydro-1*H*-pyrazol-3-yl)phenoxy)-*N*-methylpicolinamide(**8d**)

Yield: 79.3%; ESI-MS[M+H]⁺m/z:398.3; m.p.: 122.3-124.1 °C; ¹H NMR (400 MHz, DMSO-*d*₆) δ 8.82 (d, *J* = 4.7 Hz, 1H), 8.55 (d, *J* = 5.5 Hz, 1H), 7.92 (s, 1H), 7.90 (s, 1H), 7.82 (d, *J* = 7.3 Hz, 1H), 7.78 (s, 1H), 7.43 (d, *J* = 4.5 Hz, 1H), 7.43 – 7.37 (m, 2H), 7.32 (t, *J* = 9.2 Hz, 2H), 7.23 (dd, *J* = 5.5, 2.5 Hz, 1H), 5.64 (dd, *J* = 11.9, 4.8 Hz, 1H), 3.95 (d, *J* = 12.1 Hz, 1H), 3.91 (d, *J* = 12.0 Hz, 1H), 3.20 (d, *J* = 4.8 Hz, 1H), 2.78 (d, *J* = 4.7 Hz, 3H).

4-(4-(5-(2-chloro-4-fluorophenyl)-4,5-dihydro-1*H*-pyrazol-3-yl)phenoxy)-*N*-methylpicolinamide(**8e**)

Yield: 80.1%; m.p.: 112.6-113.7 °C; ESI-MS[M+H]⁺m/z: 426.2; ¹H NMR (400 MHz, DMSO-*d*₆) δ 8.80 (d, *J* = 4.9 Hz, 1H), 8.54 (d, *J* = 5.5 Hz, 1H), 7.91 (d, *J* = 8.7 Hz, 2H), 7.50 (dd, *J* = 8.8, 2.4 Hz,

1H), 7.42 (d, $J = 2.5$ Hz, 1H), 7.32 (d, $J = 8.7$ Hz, 2H), 7.22 (dd, $J = 5.6, 2.6$ Hz, 1H), 7.17 (dd, $J = 8.0, 2.1$ Hz, 1H), 7.14 (s, 1H), 5.74 (dd, $J = 12.0, 5.2$ Hz, 1H), 3.97 (dd, $J = 15.0, 11.9$ Hz, 1H), 3.14 (dd, $J = 15.2, 5.1$ Hz, 1H), 2.78 (d, $J = 4.8$ Hz, 3H)

N-methyl-4-(4-(5-(4-nitrophenyl)-4,5-dihydro-1*H*-pyrazol-3-yl)phenoxy)picolinamide(**8f**)

Yield: 78.2%; m.p.: 122.3-124.3 °C; ESI-MS[M+H]⁺m/z:418.4; ¹H NMR (400 MHz, DMSO-*d*₆) δ 8.81 (d, $J = 4.7$ Hz, 1H), 8.55 (d, $J = 5.5$ Hz, 1H), 8.27 – 8.16 (m, 2H), 7.92 (d, $J = 8.5$ Hz, 2H), 7.50 (t, $J = 10.6$ Hz, 2H), 7.42 (d, $J = 2.3$ Hz, 1H), 7.33 (t, $J = 9.1$ Hz, 2H), 7.23 (dd, $J = 5.5, 2.5$ Hz, 1H), 5.70 (dd, $J = 12.0, 5.0$ Hz, 1H), 4.02 – 3.95 (m, 1H), 3.93 (d, $J = 12.0$ Hz, 1H), 3.23 (d, $J = 5.0$ Hz, 1H), 2.78 (d, $J = 4.7$ Hz, 3H).

N-methyl-4-(4-(5-(3-nitrophenyl)-4,5-dihydro-1*H*-pyrazol-3-yl)phenoxy)picolinamide(**8g**)

Yield: 79.2%; ESI-MS[M+H]⁺m/z:418.7; m.p.: 159.7-161.2 °C; ¹H NMR (400 MHz, DMSO-*d*₆) δ 8.80 (s, 1H), 8.55 (d, $J = 5.2$ Hz, 1H), 8.14 (d, $J = 6.9$ Hz, 1H), 8.09 (s, 1H), 7.93 (d, $J = 8.3$ Hz, 2H), 7.72 – 7.60 (m, 2H), 7.43 (s, 1H), 7.34 (d, $J = 8.3$ Hz, 2H), 7.24 (s, 1H), 5.74 (d, $J = 6.9$ Hz, 1H), 3.95 (dd, $J = 15.2, 12.4$ Hz, 1H), 3.29 – 3.24 (m, 1H), 2.79 (d, $J = 4.7$ Hz, 3H).

4-(4-(5-(4-methoxyphenyl)-4,5-dihydro-1*H*-pyrazol-3-yl)phenoxy)-*N*-methylpicolinamide (**8h**)

Yield: 74.5%; ESI-MS[M+H]⁺m/z:403.5; m.p.: 134.7-135.6 °C; ¹H NMR (400 MHz, DMSO-*d*₆) δ 8.80 (d, $J = 4.6$ Hz, 1H), 8.55 (d, $J = 5.6$ Hz, 1H), 7.92 (d, $J = 8.5$ Hz, 2H), 7.44 (s, 1H), 7.33 (d, $J = 8.6$ Hz, 2H), 7.25 – 7.19 (m, 1H), 7.13 (d, $J = 8.5$ Hz, 2H), 6.89 (d, $J = 8.3$ Hz, 2H), 5.51 (dd, $J = 11.7, 3.8$ Hz, 1H), 3.91 – 3.81 (m, 1H), 3.72 (s, 3H), 3.17 (dd, $J = 15.2, 4.5$ Hz, 1H), 2.79 (d, $J = 4.7$ Hz, 3H).

N-methyl-4-(4-(5-phenyl-4,5-dihydro-1*H*-pyrazol-3-yl)phenoxy)picolinamide(**8i**)

Yield: 79.1%; ESI-MS[M+H]⁺m/z:373.1; m.p.: 133.5-134.7 °C; ¹H NMR (400 MHz, DMSO-*d*₆) δ 8.80 (s, 1H), 8.55 (d, $J = 5.5$ Hz, 1H), 7.92 (d, $J = 8.7$ Hz, 2H), 7.44 (s, 1H), 7.34 (s, 2H), 7.32 (s, 2H), 7.29 – 7.24 (m, 1H), 7.23 (d, $J = 5.7$ Hz, 2H), 7.20 (s, 1H), 5.56 (d, $J = 7.7$ Hz, 1H), 3.90 (dd, $J = 15.0, 12.0$ Hz, 1H), 3.19 (d, $J = 15.1$ Hz, 1H), 2.79 (d, $J = 4.7$ Hz, 3H).

4-(4-(5-(3,4-dichlorophenyl)-4,5-dihydro-1*H*-pyrazol-3-yl)phenoxy)-*N*-methylpicolinamide(**8j**)

Yield: 79.1%; ESI-MS[M+H]⁺m/z:442.5; m.p.: 93.7-94.6 °C; ¹H NMR (400 MHz, DMSO-*d*₆) δ 8.80 (d, *J* = 5.3 Hz, 1H), 8.55 (d, *J* = 5.6 Hz, 1H), 7.91 (d, *J* = 8.4 Hz, 2H), 7.60 (d, *J* = 8.2 Hz, 1H), 7.52 (s, 1H), 7.43 (s, 1H), 7.34 (d, *J* = 8.2 Hz, 2H), 7.22 (t, *J* = 8.1 Hz, 2H), 5.57 (dd, *J* = 11.9, 4.8 Hz, 1H), 3.89 (dd, *J* = 14.1, 11.9 Hz, 1H), 3.27 (dd, *J* = 15.2, 4.7 Hz, 1H), 2.79 (d, *J* = 4.6 Hz, 3H)

4-(4-(5-(4-fluorophenyl)-4,5-dihydro-1*H*-pyrazol-3-yl)phenoxy)-*N*-methylpicolinamide(**8k**)

Yield:72.8%; ESI-MS[M+H]⁺m/z:391.3; m.p.: 201.1-202.3 °C; ¹H NMR (400 MHz, DMSO-*d*₆) δ 8.81 (s, 1H), 8.55 (d, *J* = 5.5 Hz, 1H), 7.92 (d, *J* = 8.6 Hz, 2H), 7.43 (s, 1H), 7.33 (d, *J* = 8.2 Hz, 2H), 7.30 – 7.25 (m, 2H), 7.24 (d, *J* = 6.9 Hz, 1H), 7.16 (t, *J* = 8.6 Hz, 2H), 5.57 (d, *J* = 7.6 Hz, 1H), 3.93 – 3.83 (m, 1H), 3.20 (dd, *J* = 15.1, 4.3 Hz, 1H), 2.79 (d, *J* = 4.5 Hz, 3H).

4-(4-(5-(4-bromophenyl)-4,5-dihydro-1*H*-pyrazol-3-yl)phenoxy)-*N*-methylpicolinamide(**8i**)

Yield:75.6%; ESI-MS[M+H]⁺m/z:452.3; m.p.:138.3-138.7 °C; ¹H NMR (400 MHz, DMSO-*d*₆) δ 8.80 (s, 1H), 8.55 (d, *J* = 5.5 Hz, 1H), 7.91 (d, *J* = 8.6 Hz, 2H), 7.53 (d, *J* = 8.3 Hz, 2H), 7.43 (d, *J* = 2.5 Hz, 1H), 7.33 (d, *J* = 8.6 Hz, 2H), 7.22 (dd, *J* = 5.5, 2.6 Hz, 1H), 7.18 (d, *J* = 8.4 Hz, 2H), 5.54 (dd, *J* = 11.6, 4.6 Hz, 1H), 3.89 (dd, *J* = 15.2, 11.9 Hz, 1H), 3.20 (dd, *J* = 15.0, 4.5 Hz, 1H), 2.78 (d, *J* = 4.8 Hz, 3H).

N-methyl-4-(4-(5-(2,3,4-trimethoxyphenyl)-4,5-dihydro-1*H*-pyrazol-3-yl)phenoxy)picolinamide (**8m**)

Yield:73.6%; ESI-MS[M+H]⁺m/z:463.4; m.p.:140.0-142.1°C; ¹H NMR (400 MHz, DMSO-*d*₆) δ 8.80 (s, 1H), 8.54 (d, *J* = 5.1 Hz, 1H), 7.90 (d, *J* = 7.5 Hz, 2H), 7.44 (s, 1H), 7.31 (d, *J* = 7.5 Hz, 2H), 7.19 (t, *J* = 16.8 Hz, 1H), 6.78 – 6.65 (m, 2H), 5.57 (dd, *J* = 14.7, 13.9 Hz, 1H), 3.78 (d, *J* = 13.3 Hz, 1H), 2.77 (t, *J* = 13.9 Hz, 3H).

4-(4-(5-(2,3-dichlorophenyl)-4,5-dihydro-1*H*-pyrazol-3-yl)phenoxy)-*N*-methylpicolinamide (**8n**)

Yield:71.3%; ESI-MS[M+H]⁺m/z:442.1; m.p.:142.5-143.6°C; ¹H NMR (400 MHz, CDCl₃) δ 9.83 (s, 1H), 8.57 (d, *J* = 5.9 Hz, 1H), 7.99 (d, *J* = 13.8 Hz, 1H), 7.90 (d, *J* = 8.2 Hz, 2H), 7.38 (dd, *J* = 15.6, 7.0 Hz, 2H), 7.22 (d, *J* = 8.2 Hz, 2H), 7.19 – 7.14 (m, 1H), 6.99 (d, *J* = 7.6 Hz, 1H), 5.98 (dd, *J* = 11.9, 4.7 Hz, 1H), 3.95 – 3.81 (m, 1H), 2.49 (d, *J* = 7.7 Hz, 3H).

5.5 4-(4-formylphenoxy)-*N*-methylpicolinamide(**6**)

Benzaldehyde(10 mmol) and potassium tert-butoxide(20 mmol) were dissolved in 30 ml DMF . Then 4-(4-acetylphenoxy)-*N*-methylpicolinamide(10 mmol) was added. The mixture was refluxed for 15h. The reaction mixture was cooled and cold water was added. The precipitate of

4-(4-formylphenoxy)-*N*-methylpicolinamide(**6**) formed was filtered and recrystallized from isopropanol. Yiled: 38%.

5.6 General procedure for the preparation of compounds **7a–c**

A mixture of substituted acetophenone (0.67 mmol), NaH (1.34 mmol) and THF (10 ml) was stirred at room temperature for 1h. At the same time 4-(4-formylphenoxy)-*N*-methylpicolinamide (0.67 mmol) was dissolved in methanol(10 mL) .One hour later the latter mixture was added slowly with vigorous stirring in the former one. The mixture was kept for 8 hours. The solid formed was filtered. No further purification was needed and products were used such as were obtained.

5.7 General procedure for the preparation of compounds **9a–c**

Compounds **7a–c** (0.24 mmol) and hydrazine hydrate (2.2 mmol) were dissolved in acetic acid (10mL). The mixture was refluxed for 2 h with constant stirring. The progress of the reaction was monitored through TLC. After completion of reaction, mixture was cooled and poured into water, and it was neutralized with potassium carbonate, then it was filtered through vacuum by washing with water.

N-methyl-4-(4-(3-(4-nitrophenyl)-4,5-dihydro-1*H*-pyrazol-5-yl)phenoxy) picolinamide (**9a**)

Yield:73.2%; ESI-MS[M+H]⁺m/z:418.5; m.p.:151.2-152 °C; ¹H NMR (400 MHz, DMSO-*d*₆) δ 8.78 (s, 1H), 8.51 (d, *J* = 5.5 Hz, 1H), 8.31 (d, *J* = 8.4 Hz, 2H), 8.05 (d, *J* = 8.5 Hz, 2H), 7.41 – 7.35 (m, 2H), 7.34 – 7.31 (m, 1H), 7.22 – 7.17 (m, 2H), 7.16 – 7.11 (m, 1H), 5.67 (d, *J* = 7.1 Hz, 1H), 4.36 (t, *J* = 4.8 Hz, 2H), 3.96 (dd, *J* = 17.7, 12.0 Hz, 1H), 2.78 (d, *J* = 4.5 Hz, 3H).

4-(4-(3-(4-bromophenyl)-4,5-dihydro-1*H*-pyrazol-5-yl)phenoxy)-*N*-methylpicolinamide(**9b**)

Yield:75.2%; ESI-MS[M+H]⁺m/z:452.5; m.p.:155.8-156.4 °C; ¹H NMR (400 MHz, DMSO-*d*₆) δ 8.77 (d, *J* = 4.5 Hz, 1H), 8.51 (d, *J* = 5.5 Hz, 1H), 7.75 (d, *J* = 8.3 Hz, 2H), 7.68 (d, *J* = 8.2 Hz, 2H), 7.39 (s, 1H), 7.33 (d, *J* = 8.2 Hz, 2H), 7.18 (d, *J* = 8.1 Hz, 2H), 7.15 (d, *J* = 5.3 Hz, 1H), 5.62 (dd, *J* = 11.9, 4.4 Hz, 1H), 4.37 (s, 2H), 3.88 (dd, *J* = 17.9, 12.0 Hz, 1H), 2.78 (d, *J* = 4.7 Hz, 3H).

4-(4-(3-(4-chlorophenyl)-4,5-dihydro-1*H*-pyrazol-5-yl)phenoxy)-*N*-methylpicolinamide(**9c**)

Yield:76.9%; ESI-MS[M+H]⁺m/z:408.5; m.p.:159.3-160.6°C; ¹H NMR (400 MHz, DMSO-*d*₆) δ 8.77 (s, 1H), 8.51 (s, 1H), 7.81 (t, *J* = 9.4 Hz, 3H), 7.54 (d, *J* = 6.9 Hz, 3H), 7.39 (s, 1H), 7.33 (d, *J* = 7.5 Hz, 2H), 7.22 – 7.12 (m, 3H), 6.97 (d, *J* = 8.3 Hz, 1H), 5.62 (s, 1H), 4.36 (s, 2H), 3.94 – 3.79 (m, 1H), 2.78 (s, 3H)

5.8 General procedure for the preparation of compounds **10a–e**, **11a**

A mixture of compounds **5a–e** or **7a** (0.26 mmol), thiosemicarbazide (0.29 mmol) and potassium hydroxide (0.31 mmol) in ethanol (6mL) was submitted to microwave irradiation for 15 min at a power of 100 W and a temperature of 60 °C. The progress of the reaction was monitored through TLC. The reaction mixture was cooled and cold water was added. The compound was filtered and recrystallized from ethanol.

4-(4-(1-carbamothioyl-5-(3-nitrophenyl)-4,5-dihydro-*1H*-pyrazol-3-yl)phenoxy)-*N*-methylpicolinamide (**10a**)

Yield:69.9%; ESI-MS[M+H]⁺m/z:477.5; m.p.:108.5-110.6°C; ¹H NMR (400 MHz, DMSO-*d*₆) δ 8.78 (d, *J* = 4.3 Hz, 1H), 8.54 (d, *J* = 5.4 Hz, 1H), 8.19 (s, 1H), 8.16 – 8.07 (m, 2H), 8.02 (d, *J* = 8.8 Hz, 2H), 7.64 (d, *J* = 6.0 Hz, 2H), 7.43 (s, 1H), 7.33 (d, *J* = 8.6 Hz, 2H), 7.22 (d, *J* = 5.6 Hz, 1H), 6.10 (d, *J* = 10.6 Hz, 1H), 4.00 (dd, *J* = 15.4, 11.8 Hz, 1H), 3.28 (s, 1H), 2.78 (d, *J* = 4.6 Hz, 3H).

4-(4-(1-carbamothioyl-5-(4-fluorophenyl)-4,5-dihydro-*1H*-pyrazol-3-yl)phenoxy)-*N*-methylpicolinamide (**10b**)

Yield:65.9%; ESI-MS[M+H]⁺m/z:450.7; m.p.:102.4-103.9°C; ¹H NMR (400 MHz, DMSO-*d*₆) δ 8.80 (d, *J* = 4.8 Hz, 1H), 8.54 (d, *J* = 5.6 Hz, 1H), 8.07 (s, 1H), 8.02 (d, *J* = 8.6 Hz, 2H), 7.97 (s, 1H), 7.44 (t, *J* = 7.3 Hz, 1H), 7.32 (d, *J* = 8.7 Hz, 2H), 7.22 (dd, *J* = 5.7, 2.7 Hz, 1H), 7.20 – 7.16 (m, 2H), 7.13 (d, *J* = 8.9 Hz, 1H), 5.93 (dd, *J* = 11.4, 3.3 Hz, 1H), 4.12 (dd, *J* = 10.6, 5.3 Hz, 1H), 3.93 (dd, *J* = 15.3, 11.7 Hz, 1H), 3.22 (d, *J* = 3.6 Hz, 1H), 2.78 (d, *J* = 4.8 Hz, 2H).

4-(4-(1-carbamothioyl-5-(4-chlorophenyl)-4,5-dihydro-*1H*-pyrazol-3-yl)phenoxy)-*N*-methylpicolinamide(**10c**)

Yield:63.6%; ESI-MS[M+H]⁺m/z:466.3; m.p.:105.1-106.4°C; ¹H NMR (400 MHz, DMSO-*d*₆) δ 8.77 (d, *J* = 4.6 Hz, 1H), 8.51 (d, *J* = 5.5 Hz, 1H), 8.11 (s, 1H), 8.01 (s, 1H), 7.94 (t, *J* = 8.3 Hz, 2H), 7.53 (d, *J* = 8.2 Hz, 2H), 7.40 (s, 1H), 7.27 (d, *J* = 8.2 Hz, 2H), 7.17 (d, *J* = 8.3 Hz, 2H), 7.16 – 7.10 (m, 1H), 5.98 (d, *J* = 11.5 Hz, 1H), 3.93 (dd, *J* = 15.0, 11.7 Hz, 1H), 3.27 (s, 1H), 2.77 (d, *J* = 4.7 Hz, 3H).

4-(4-(1-carbamothioyl-5-(2,3-dichlorophenyl)-4,5-dihydro-*1H*-pyrazol-3-yl)phenoxy)-*N*-methylpicolinamide(**10d**)

Yield:70.3%; ESI-MS[M+H]⁺m/z:500.4; m.p.:107.5-108.8°C; ¹H NMR (400 MHz, DMSO-*d*₆) δ 8.79 (d, *J* = 4.5 Hz, 1H), 8.52 (t, *J* = 12.6 Hz, 1H), 8.23 (s, 1H), 8.09 (s, 1H), 8.01 (d, *J* = 8.3 Hz, 2H), 7.55 (d, *J* = 7.9 Hz, 1H), 7.40 (d, *J* = 18.4 Hz, 1H), 7.34 (d, *J* = 6.0 Hz, 1H), 7.32 (s, 1H), 7.30 (s, 1H), 7.26 – 7.15 (m, 1H), 6.93 (s, 1H), 6.18 (d, *J* = 7.8 Hz, 1H), 4.04 (dd, *J* = 15.1, 12.1 Hz, 1H), 3.20 (d, *J* = 14.0 Hz, 1H), 2.78 (d, *J* = 4.5 Hz, 3H).

4-(4-(1-carbamothioyl-5-(4-cyanophenyl)-4,5-dihydro-1*H*-pyrazol-3-yl)phenoxy)-*N*-methylpicolinamide(**10e**)

Yield:71.2%; ESI-MS[M+H]⁺m/z:457.2; m.p.:98.7-100.2°C; ¹H NMR (400 MHz, DMSO-*d*₆) δ 8.79 (d, *J* = 4.6 Hz, 1H), 8.54 (d, *J* = 5.6 Hz, 1H), 8.16 (s, 1H), 8.01 (d, *J* = 8.6 Hz, 2H), 7.80 (d, *J* = 8.2 Hz, 2H), 7.43 (t, *J* = 8.7 Hz, 1H), 7.35 (s, 1H), 7.34 – 7.29 (m, 2H), 7.24 – 7.17 (m, 1H), 6.07 – 5.93 (m, 1H), 4.12 (d, *J* = 5.2 Hz, 1H), 3.97 (dd, *J* = 15.1, 11.8 Hz, 1H), 3.27 – 3.19 (m, 1H), 2.78 (d, *J* = 4.8 Hz, 3H).

4-(4-(1-carbamothioyl-3-(4-nitrophenyl)-4,5-dihydro-1*H*-pyrazol-5-yl)phenoxy)-*N*-methylpicolinamide(**11a**)

Yield:65.8%; ESI-MS[M+H]⁺m/z:447.2; m.p.:118.4-120.1°C; ¹H NMR (400 MHz, DMSO-*d*₆) δ 8.78 (s, 1H), 8.64 – 8.47 (m, 1H), 8.29 (d, *J* = 8.2 Hz, 1H), 8.16 (d, *J* = 8.7 Hz, 2H), 8.07 (d, *J* = 9.5 Hz, 1H), 7.95 (d, *J* = 8.2 Hz, 1H), 7.41 (d, *J* = 8.9 Hz, 2H), 7.28 (d, *J* = 8.6 Hz, 2H), 7.18 (d, *J* = 7.5 Hz, 1H), 7.13 (d, *J* = 3.0 Hz, 1H), 6.03 (d, *J* = 11.5 Hz, 1H), 4.20 – 4.08 (m, 1H), 3.99 (dd, *J* = 15.0, 11.4 Hz, 1H), 2.77 (d, *J* = 5.0 Hz, 3H).

5.9 Cytotoxicity assay *in vitro*

The cytotoxic activities of compounds were evaluated by A549, PC-3, HepG2 and MCF-7 cell lines by the standard MTT assay *in vitro*, with VEGFR2/KDR inhibitors sorafenib as positive control. The cancer cell lines were cultured in minimum essential medium (MEM) supplement with 10% fetal bovine serum (FBS). Approximately 4×10³ cells, suspended in MEM medium, were plated onto each well of a 96-well plate and incubated in 5% CO₂ at 37 °C for 24 h. The test compounds at indicated final concentrations were added into the culture medium and the cell cultures were continued for 72 h. Fresh MTT was added to each well at a terminal concentration of 5μg/mL and incubated with cells at 37°C for 4 h. The formazan crystals were dissolved in 100 μL DMSO each well, and the absorbency at 492 nm (for absorbance of MTT formazan) and 630 nm (for the reference wavelength) was measured by the ELISA reader. The initial concentration of the compound was 100 ug/mL, which was three times dilution and diluted six times. That is to say, we tested seven concentrations of each compound. And all the compounds were tested three times in each of the cell lines. The results expressed as inhibition rates or IC₅₀ (half-maximal inhibitory concentration) were the averages of two determinations and calculated by using the Bacus Laboratories Incorporated Slide Scanner (Bliss) software.

5.10 Tyrosine kinases assay *in vitro*

The selected compounds (**8b**, **8h**, **8i** and **9a**) are tested for their activity against one or several tyrosine kinases (VEGFR-2/KDR, BRAF, CRAF, c-Met, EGFR and Flt-3 kinases) through the mobility shift assay together with reference compounds Sorafenib and staurosporine. All kinase assays were performed on 384-well plates in a 50 μ L reaction volume. The kinase base buffer contains 50 mM HEPES, pH 7.5, 10 mM MgCl₂, 0.0015% Brij-35 and 2 mM DTT. The stop buffer contains 100mM HEPES, pH 7.5, 0.015% Brij-35, 0.2% Coating Reagent #3 and 50 mM EDTA. The compounds were diluted to 500 μ M by 100% DMSO, then 10 μ L of compound was transferred to a new 96-well plate as the intermediate plate, and 90 μ L kinase buffer was added to each well. 5 μ L of each well of the intermediate plate was transferred to 384-well plates. The following amounts of enzyme and substrate were used per well: kinase base buffer, FAM-labeled peptide, ATP and enzyme solution. Wells containing the substrate, enzyme, DMSO without compound were used as DMSO control. Wells containing substrate without enzyme were used as low control and then incubated at room temperature for 10 min. 10 μ L peptide solution was added to each well. Incubated at 28 °C for specified period of time and stopped reaction by 25 μ L stop buffer. At last, collected data on Caliper program and converted conversion values to inhibition values. Percent inhibition = $(\text{max-conversion}) / (\text{max-min}) * 100$. “max” denotes DMSO control; “min” denotes low control. It was tested by Shanghai ChemPartners.

5.11 Cell apoptosis assay by flow cytometry

A549 cells were seeded in 16-well plates at a density of 1×10^6 cells/well in RPMI 1640 medium and treated with 3, 6 and 12 μ M concentration of **8b** for 48 h. Cultured cells were stained with Annexin VFITC and propidium iodide (PI) in the dark at 4 °C for 30 min and analyzed by FACS Calibur flow cytometer (Becton Dickinson, San Jose, CA) using Cell Quest software^[23].

5.12 Docking studies

For docking purposes, the three-dimensional structure of the VEGFR2/KDR (PDB code: 4ASD) and c-Met (PDB code: 3LQ8) were obtained from RCSB Protein Data Bank. Autodock Vina 1.12, Discover Studio 3.5 visualizer and Open Babel were used for the docking study. Firstly, using the Discover Studio 3.5 visualizer to prepare ligands (**8b**) and acceptor protein (PDB code: 4ASD and 3LQ8), then saved as pdb format after energy minimization for ligand and clean protein, defined the activity site for acceptor protein. Secondly, the pdb file of ligand and acceptor protein were converted to the pdbqt format by the Open Babel tool. Thirdly, docking was carried out by uploading

the pdbqt file to the Autodock vina 1.1.2, and the result was named out.pdbq. Moreover, out.pdbqt file was uploaded to the Discover Studio 3.5 visualizer for analyzing the result.

Acknowledgments

We gratefully acknowledge the generous support provided by The National Natural Science Funds, China (No. 21662014), Outstanding Youth Foundation of Jiangxi, Natural Science Foundation of Jiangxi, China (20171BCB23078), Natural Science Foundation of Jiangxi, China (20171ACB21052 & 20171BAB215073), Science and Technology Project Founded by the Education Department of Jiangxi Province (GJJ160787)

References and notes

- [1]. Jemal A, Bray F, Center M M, et al. Global cancer statistics[J]. CA: a cancer journal for clinicians, 2011, 61(2): 69-90.
- [2]. Yang Y S, Li Q S, Sun S, et al. Design, modification and 3D QSAR studies of novel 2, 3-dihydrobenzo [b][1, 4] dioxin-containing 4, 5-dihydro-1H-pyrazole derivatives as inhibitors of B-Raf kinase[J]. Bioorganic & medicinal chemistry, 2012, 20(20): 6048-6058.
- [3] Machado V A, Peixoto D, Costa R, et al. Synthesis, antiangiogenesis evaluation and molecular docking studies of 1-aryl-3-[(thieno [3, 2-b] pyridin-7-ylthio) phenyl] ureas: Discovery of a new substitution pattern for type II VEGFR-2 Tyr kinase inhibitors[J]. Bioorganic & medicinal chemistry, 2015, 23(19): 6497-6509.
- [4] Peyssonnaud C, Eychène A. The Raf/MEK/ERK pathway: new concepts of activation[J]. Biology of the Cell, 2001, 93(1-2): 53-62.
- [5] Lu W, Li P, Shan Y, et al. Discovery of biphenyl-based VEGFR-2 inhibitors. Part 3: design, synthesis and 3D-QSAR studies[J]. Bioorganic & medicinal chemistry, 2015, 23(5): 1044-1054.
- [6] Ling Y, Wang Z, Zhu H, et al. Synthesis and biological evaluation of farnesylthiosalicylamides as potential anti-tumor agents[J]. Bioorganic & medicinal chemistry, 2014, 22(1): 374-380.
- [7] Wang W, Wu C, Wang J, et al. Synthesis, activity and docking studies of phenylpyrimidine-carboxamide Sorafenib derivatives[J]. Bioorganic & Medicinal Chemistry, 2016, 24(23): 6166-6173.
- [8] Machado V A, Peixoto D, Costa R, et al. Synthesis, antiangiogenesis evaluation and molecular docking studies of 1-aryl-3-[(thieno [3, 2-b] pyridin-7-ylthio) phenyl] ureas: Discovery of a new substitution pattern for type II VEGFR-2 Tyr kinase inhibitors[J]. Bioorganic & medicinal chemistry,

2015, 23(19): 6497-6509.

[9] Kamal A, Faazil S, Ramaiah M J, et al. Synthesis and study of benzothiazole conjugates in the control of cell proliferation by modulating Ras/MEK/ERK-dependent pathway in MCF-7 cells[J]. *Bioorganic & medicinal chemistry letters*, 2013, 23(20): 5733-5739.

[10]. Cottineau B, Toto P, Marot C, et al. Synthesis and hypoglycemic evaluation of substituted pyrazole-4-carboxylic acids[J]. *Bioorganic & medicinal chemistry letters*, 2002, 12(16): 2105-2108.

[11]. Ranatunge R R, Garvey D S, Janero D R, et al. Synthesis and selective cyclooxygenase-2 (COX-2) inhibitory activity of a series of novel bicyclic pyrazoles[J]. *Bioorganic & medicinal chemistry*, 2004, 12(6): 1357-1366.

[12] Koca I, Özgür A, Coşkun K A, et al. Synthesis and anticancer activity of acyl thioureas bearing pyrazole moiety[J]. *Bioorganic & medicinal chemistry*, 2013, 21(13): 3859-3865.

[13]. Manna F, Chimenti F, Fioravanti R, et al. Synthesis of some pyrazole derivatives and preliminary investigation of their affinity binding to P-glycoprotein[J]. *Bioorganic & medicinal chemistry letters*, 2005, 15(20): 4632-4635.

[14]. Zhang J, Shen B, Lin A. Novel strategies for inhibition of the p38 MAPK pathway[J]. *Trends in pharmacological sciences*, 2007, 28(6): 286-295.

[15]. Li M, Liu C L, Yang J C, et al. Synthesis and Biological Activity of New (E)- α -(Methoxyimino) benzeneacetate Derivatives Containing a Substituted Pyrazole Ring†[J]. *Journal of agricultural and food chemistry*, 2009, 58(5): 2664-2667.

[16]. Cole L M, Nicholson R A, Casida J E. Action of phenylpyrazole insecticides at the GABA-gated chloride channel [J]. *Pesticide Biochemistry and Physiology*, 1993, 46(1): 47-54.

[17]. Montoya A, Quiroga J, Abonia R, et al. Synthesis and in vitro antitumor activity of a novel series of 2-pyrazoline derivatives bearing the 4-aryloxy-7-chloroquinoline fragment[J]. *Molecules*, 2014, 19(11): 18656-18675.

[18] Reddy, M.V.R.; Billa, V.K.; Pallela, V.R.; Mallireddigari, M.R.; Boominathan, R.; Gabriel, J.L.; Reddy, E.P. Design, synthesis, and biological evaluation of 1-(4-sulfamylphenyl)-3-trifluoromethyl-5-indolyl pyrazolines as cyclooxygenase-2 (COX-2) and lipoxygenase (LOX) inhibitors. *Bioorg. Med. Chem.* 2008, 16, 3907–3916.

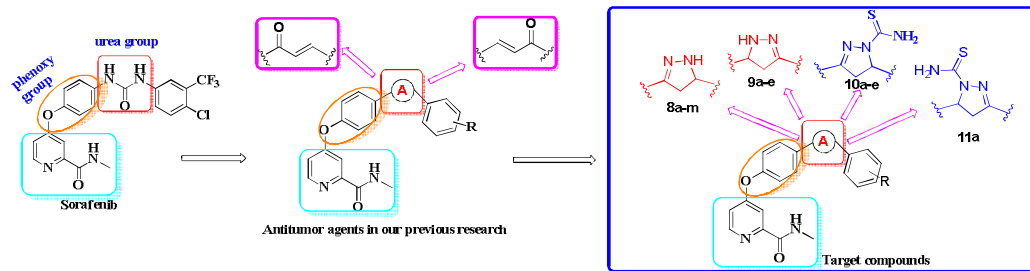
[19]. Zhu X, Li Z, Jin C, et al. Mechanically activated synthesis of 1, 3, 5-triaryl-2-pyrazolines by high speed ball milling[J]. *Green Chemistry*, 2009, 11(2): 163-165.

- [20]. Yang Y S, Li Q S, Sun S, et al. Design, modification and 3D QSAR studies of novel 2, 3-dihydrobenzo [b][1, 4] dioxin-containing 4, 5-dihydro-1*H*-pyrazole derivatives as inhibitors of B-Raf kinase[J]. Bioorganic & medicinal chemistry, 2012, 20(20): 6048-6058.
- [21]. Zhao M Y, Yin Y, Yu X W, et al. Synthesis, biological evaluation and 3D-QSAR study of novel 4, 5-dihydro-1*H*-pyrazole thiazole derivatives as BRAF V600E inhibitors[J]. Bioorganic & medicinal chemistry, 2015, 23(1): 46-54.
- [22]. Wu C, Wang M, Tang Q, et al. Design, synthesis, activity and docking study of sorafenib analogs bearing sulfonylurea unit[J]. Molecules, 2015, 20(10): 19361-19371.
- [23]. Lin F, Lin P, Zhao D, et al. Sox2 targets cyclinE, p27 and survivin to regulate androgen-independent human prostate cancer cell proliferation and apoptosis[J]. Cell Prolif. 2012 ,45(3):207.

Research Highlights

- ▶ Four series of Sorafenib derivatives bearing pyrazole scaffold (**8a–m**, **9a–c**, **10a–e** and **11a**) were synthesized and characterized.
- ▶ Most of the synthesized compounds showed moderate to significant antitumor activity.
- ▶ **8b** showed excellent cytotoxicity activity and selectivity with the IC_{50} values were equivalent to Sorafenib.
- ▶ Docking study was investigated to explore the binding modes of compounds with VEGFR and c-Met.

ACCEPTED MANUSCRIPT



ACCEPTED MANUSCRIPT